Second harmonic generation in ordered $Ga_{1-x}In_xP$

B. Fluegel, A. Mascarenhas, J. F. Geisz, and J. M. Olson
National Renewable Energy Laboratory, Golden, Colorado 80401
(Received 9 December 1997)

Reflection second harmonic generation (SHG) has been used to measure the rotation/reflection properties of spontaneously ordered $Ga_{1-x}In_xP$. Particular conditions are identified in which the SHG signal arises solely from the order-induced symmetry breaking of the 4 operation in zinc blende. By extending the usual experimental techniques to the epilayer edges, the point group of ordered $Ga_{1-x}In_xP$ was completely determined from optical methods, and the four components of the nonlinear susceptibility were measured. The case of double-variant samples is also discussed. [S0163-1829(98)51812-7]

The spontaneous ordering that occurs in $Ga_{1-x}In_xP$ results in a CuPt structure in which the cation planes alternate as Ga and In rich, approximating a monolayer superlattice. The new structure predicts changes in the optical properties, and these have been observed in the way light interacts with the lattice directly via Raman scattering,[1] or through the electronic polarizability in reflection differential spectroscopy,[2] birefringence,[3] and photoluminescence excitation.[4] Nonlinear,[5] electro-optical,[6] and elasto-optical[7] properties have been used as perturbations to study the linear susceptibility $\chi^{(1)}$, and dephasing has been measured with four-wave mixing,[8] but no previous experimental works, to the best of our knowledge, have studied the effect of ordering on the nonlinear optical properties themselves. In this paper we measure reflection second harmonic generation (SHG) in ordered $Ga_{1-x}In_xP$. SHG is technologically useful, and is also a nondestructive optical probe of the crystal structure. The linear optical properties mentioned above are determined by $\chi^{(1)}$, and hence can at most classify the crystal structure into three categories that are linear optically isotropic, uniaxial, or (possibly frequency dependent) biaxial. To get more information optically requires a property that depends, in a more complex, but well-understood way, on the structure. SHG arises from the second-order nonlinear susceptibility $\chi^{(2)}$, a third rank tensor whose 27 elements are greatly simplified by the point symmetry operations of the crystal. For example, the SHG signal will be zero if both the fundamental and the SH electric field are in a line, plane, or space that has, respectively, a one-, two-, or three-dimensional inversion symmetry. Thus SHG is sensitive to rotation and reflections properties, in contrast to electron diffraction, which shows a crystal's translational properties.

The second-harmonic polarization induced by an electric field $\vec{E}$ is simply

$$\vec{P}_{2\omega}=\vec{\vec{\chi}}^{(2)}(2\omega=\omega+\omega)\cdot\vec{E}_{\omega}\vec{E}_{\omega}. \tag{1}$$

The radiated electric field $E_{2\omega}$ that results from this polarization and exits the crystal, is detected as an irradiance that depends on many experimental details such as propagation direction, Fresnel factors, and phase matching. Without computing these details, very useful conclusions can still be made by studying SHG as a function of the rotation of the sample about its surface normal. By measuring the reflection SHG at a frequency 2ω above the band gap, multiple reflections are eliminated, and phase matching can be ignored, since the absorption depth is less than the coherence length. Furthermore, the signal magnitude can be directly compared with that of the exposed GaAs substrate since the refractive indices are nearly equal. In principle, the components of $\chi^{(2)}$ can be found by a judicious choice of the fundamental and 2ω directions. In practice, the choices are limited by the thin-film geometry, and the fact that strong single-variant ordering requires a vicinal cut substrate.

In analyzing the results, we make use of both the cubic coordinate system of the GaAs substrate, group $43m$, and the trigonal (Cartesian) coordinate system appropriate for a group $3m$ crystal. The cubic system is chosen such that the (001) surface of the substrate is tilted from the [111] direction. The trigonal system is chosen with the threefold axis in this same direction, and in the convention[9] that the x axis is normal to a mirror plane:

$$\hat{X}^{\mathrm{trig}}=\frac{1}{\sqrt{2}}(-\hat{X}^{\mathrm{cub}}-\hat{Y}^{\mathrm{cub}}),$$

$$\hat{Y}^{\mathrm{trig}}=\frac{1}{\sqrt{6}}(\hat{X}^{\mathrm{cub}}-\hat{Y}^{\mathrm{cub}}-2\hat{Z}^{\mathrm{cub}}), \tag{2}$$

$$\hat{Z}^{\mathrm{trig}}=\frac{1}{\sqrt{3}}(\hat{X}^{\mathrm{cub}}-\hat{Y}^{\mathrm{cub}}+\hat{Z}^{\mathrm{cub}}).$$

Two single-variant ordered $Ga_{1-x}In_xP$ samples were used for the bulk of this work. Both are grown using atmospheric-pressure organometallic vapor phase epitaxy on a (001) GaAs substrate cut 6° toward $\langle 111\rangle_B$. Sample 1, used for epilayer reflection, is 2 μm thick and sample 2, used for edge reflection, is 10 μm thick. The 10 K heavy-hole-like exciton energies are 1.891 and 1.909 eV.

The experimental arrangement uses high-repetition-rate ultrafast pulses, which have been shown to provide efficient SHG without heating the substrate or causing optical damage.[10] 1 mW of 76-MHz, 150-fs pulses from an 800-nm Ti sapphire oscillator was polarized and focused onto the $Ga_{1-x}In_xP$ surface. The light collected in the specular reflection was polarized, harmonically filtered, and detected with a

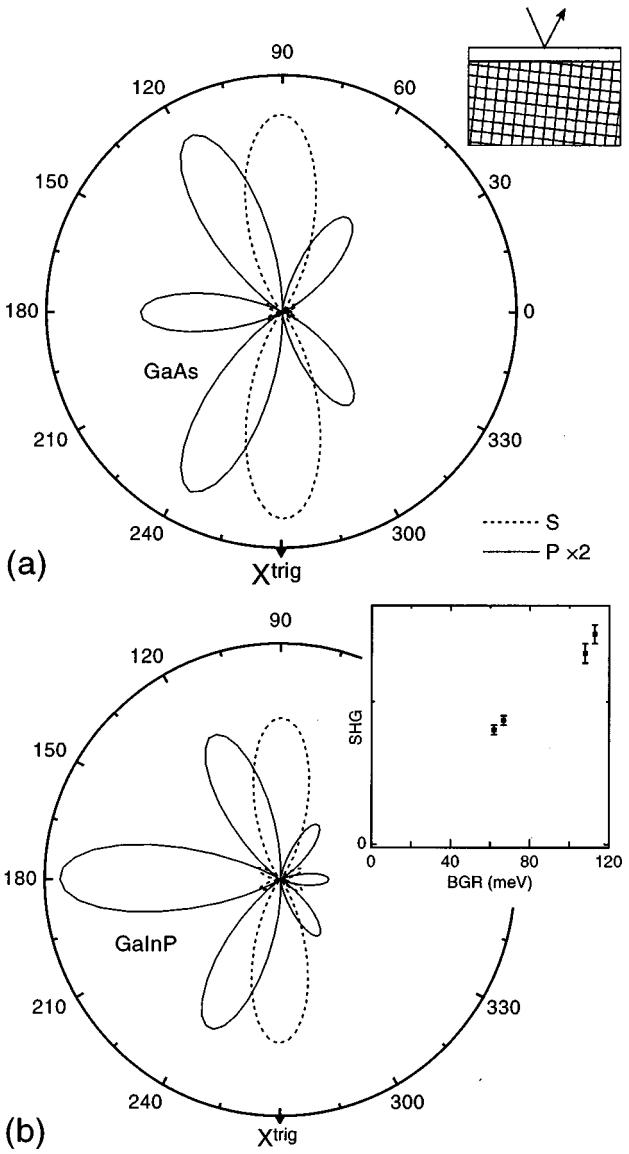

FIG. 1. SHG from the off-axis reflection on the GaAs surface (a), and the $Ga_{1-x}In_xP$ epilayer surface (b), as a function of plane of incidence rotation. The laser is *s* polarized, and the SHG is analyzed in the *s* and *p* directions, shown as dotted and solid lines. θ is the angle between the plane of incidence and the YZ^{trig} plane. Inset of (a) shows the experiment geometry for $\theta=0$. Inset of (b) shows the magnitude of the 0° $Ga_{1-x}In_xP$ peak plotted against the band-gap reduction of four samples of varying degree of order. These samples were grown in conditions similar to sample 1, but with different growth temperatures and III/V ratios. Band-gap shifts were measured in Ref. 5.

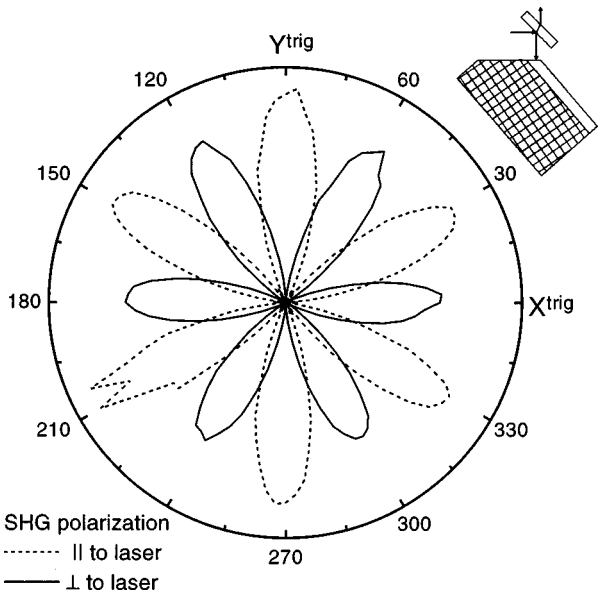

FIG. 2. SHG from the normally incident reflection of the beveled $Ga_{1-x}In_xP$ edge. SHG is analyzed parallel to (dotted line) and orthogonal to (solid line) the laser polarization. θ is the angle between the laser polarization and X^{trig}. The sharp structure is noise associated with the rough surface. The inset shows the experimental geometry.

spectrometer and multichannel charge-coupled device. Three different reflection geometries were chosen to exploit the expected high-symmetry directions. These are shown in the insets of Figs. 1–3.

a. Off-axis reflection from the 6°*B* vicinal $(0\ 0\ 1)^{\mathrm{cub}}$ surface of sample 1. The incident angle, 20.5°, was chosen such that the transmitted fundamental propagated along the $-Z^{\mathrm{cub}}$ axis. The spot size was 30 μm.

b. Normal reflection from the $(1\ 1\ \bar{1})^{\mathrm{cub}}$ plane of sample 2. This surface was exposed by mechanically beveling the film and substrate.

c. Normal reflection from the $(0\ \bar{1}\ \bar{1})^{\mathrm{cub}}$ cleaved edge of sample 2. In *b* and *c*, a reflecting objective was used to focus down to a 2-μm-diam spot.

In all geometries, the sample was rotated through an azimuthal angle θ about the surface normal and the signal was measured parallel and orthogonal to the laser polarization. Data are plotted in the reference frame of the sample, so that crystal directions can be indicated on the plot. The laser spot was centered on the rotation axis to within one spot size. The SHG efficiency is typically homogeneous over much larger areas.

Results of geometry *a* for an *s*-polarized fundamental are shown in Fig. 1 for $Ga_{1-x}In_xP$ and for a bare 6°*B* GaAs substrate. In both cases, the largest signals come from the off-axis laser accessing the $\chi^{(2)\mathrm{cub}}_{123}$ of GaAs, and equivalent elements in $Ga_{1-x}In_xP$. To clearly see the effect of ordering in SHG, we must look in the directions forbidden by the symmetry operations of GaAs, i.e., group $\bar{4}3m$. At $\theta=0°$ in Fig. 1(a), all vectors in Eq. (1) are in the XY^{cub} plane, which has a two-dimensional inversion symmetry, giving zero SHG for GaAs. The orthogonal polarized peak of $Ga_{1-x}In_xP$ in Fig. 1(b) shows that this symmetry operation, the fourfold inversion axis, is broken. The inset shows the magnitude of this peak, normalized to the 180° peak, for several samples of varying degrees of ordering, plotted against their low-temperature band-gap reduction. The amount of SHG in this zinc-blende-forbidden direction increases monotonically with band-gap reduction, and hence with ordering, although we expect no simple dependence on the ordering parameter.

By accessing special crystal directions where the SHG is zero, we can identify the precise point group of ordered $Ga_{1-x}In_xP$ using only optical measurements. For example, the dashed curve of Fig. 1(b) shows that the *s*-polarization SHG is zero at $\theta=0$, and therefore $\chi^{(2)\mathrm{trig}}_{111}=0$. Analyzing further $\chi^{(2)}$ components requires studying the edge

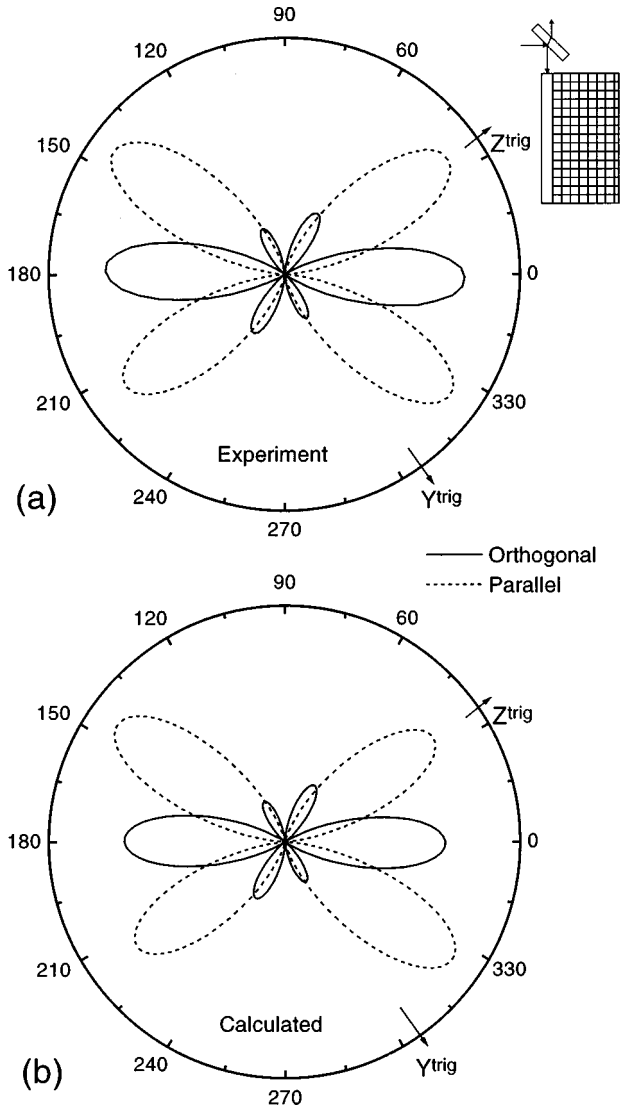

FIG. 3. (a) SHG from the normally incident reflection of the cleaved $Ga_{1-x}In_xP$ edge. SHG is analyzed parallel to (dotted line) and orthogonal to (solid line) the laser polarization. The inset shows the experimental geometry. (b) Calculated $|P|^2$ using Eq. (1), and the measured $\chi^{(2)}$ results in Table I for P parallel to (dotted line) and orthogonal to (solid line) the laser.

geometries *b* and *c*. In the results of *b*, shown in Fig. 2, we see that X^{trig} is one of three special directions in that no SHG is generated in this direction by either laser polarization, and thus $\chi_{122}^{(2)\text{trig}}=\chi_{111}^{(2)\text{trig}}=0$. While $\chi_{133}^{(2)\text{trig}}$ is not directly accessible, we used geometry *a* with a *p*-polarized laser and multiple incident angles to obtain $\chi_{133}^{(2)\text{trig}}=\chi_{123}^{(2)trig}=0$. These four results are summarized in the SHG matrix notation of Fig. 4(a). The lowest point symmetry operation mandating this is a mirror plane perpendicular to X^{trig}.

In addition to the mirror plane, the other symmetry operation that would be present in a $3m$ crystal is a threefold rotation axis. Figure 2 shows a sixfold rotation symmetry about the Z^{trig} axis. A sixfold rotation symmetry in the crystal structure would result in a zero SHG signal, thus the pattern observed in the irradiance must indicate a threefold rotation symmetry in the field. However, this measurement is

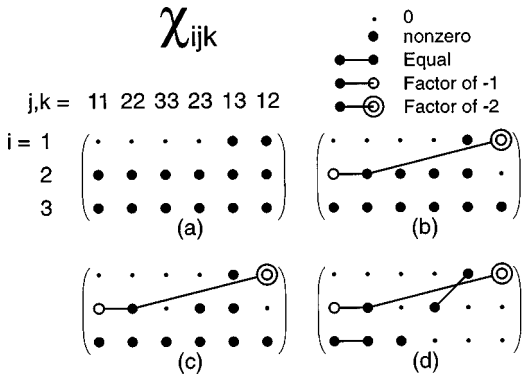

FIG. 4. Diagrams showing the relationships between components of $\chi^{(2\omega)}$ using the contracted matrix notation of Ref. 9. (a) Experimental results from the zero signals of Figs. 1 and 2. (b) Summary including the results from the two-dimensional threefold rotation of Fig. 2. (c) Summary including the result from 3(a). (d) The required form for a crystal of symmetry $3m$.

performed entirely in the XY^{trig} plane, and thus gives no information about the Z^{trig} direction. Demonstration of complete threefold symmetry of the $\chi^{(2)}$ tensor would require an off-normal, rotating measurement of the beveled edge sample. Working only with the two-dimensional rotation, we have the symmetry elements summarized in Fig. 4(b). Finally, Fig. 3(a) shows the cleaved edge geometry *c* that accesses the directions Y^{trig} and Z^{trig}. The zero orthogonal signal at $\theta=35°$ (laser parallel to Z^{trig}) gives $\chi_{233}^{(2)\text{trig}}=0$, and this datum is added to Fig. 4(c). The lowest symmetry point group including these components is $3m$, shown in Fig. 4(d). We note that, generally, the crystal structure determines only the *minimum* symmetry elements of optical properties such as $\chi^{(2)}$. Thus it would be possible for an unknown sample to belong to a lower group, yet its optical properties could have additional elements unrelated to its group, such as Kleinman symmetry. However, the usual conditions for this are avoided by using a SHG energy above the band gap. Furthermore, additional information is available from $\chi^{(1)}$: birefringence measurements prove that ordered $Ga_{1-x}In_xP$ is a uniaxial crystal,[11,3] thus eliminating the cubic, triclinic, monoclinic, and orthorhombic systems. The two remaining classes that can include the elements of Fig. 4(c) are $3m$ and $\bar{6}2m$; the latter is easily dismissed by the form of Fig. 3(a).

Thus the point group of ordered $Ga_{1-x}In_xP$ can be completely identified by optical, nondestructive methods. With the point group known, i.e., Fig. 4(d) the magnitudes of the four independent elements of $\chi^{(2)}$ for $Ga_{1-x}In_xP$ can be estimated for sample 2. In geometries *b* and *c*, we can quantitatively compare the SHG signal of $Ga_{1-x}In_xP$ with that of the nearby GaAs substrate under identical experimental conditions. Since the two materials also have similar refractive indices, the ratio of GaAs to $Ga_{1-x}In_xP$ peaks can be related to their relative $|\chi^{(2)}|^2$. In this way, the magnitudes are found relative to $\chi_{123}^{(2)\text{GaAs}}$, and phases between elements were checked by fitting to the curves of Fig. 3(a). Good agreement is found with all elements real, as shown in the calculated curve of Fig. 3(b). In the limit of zero ordering, the coefficients must revert to the form of group $\bar{4}3m$. Table I lists the measured values next to their equivalent analytical

TABLE I. First column: components of the second-order nonlinear susceptibility measured in $Ga_{1-x}In_xP$ sample 2. Last column: analytical components for GaAs, computed from the single nonzero cubic component (Ref. 9) and the coordinate transformation in Eq. (2). All are expressed in units of $\chi^{(2)\mathrm{cub}}_{123}$ for GaAs. A phase factor common to column 1 is undetermined.

	$Ga_{1-x}In_xP$ (measured)	GaAs (analytical)
$\chi^{\mathrm{trig}}_{113}$	0.57 ± 0.07	$\frac{1}{\sqrt{3}}=0.58$
$\chi^{\mathrm{trig}}_{211}$	-0.75 ± 0.05	$-\sqrt{\frac{2}{3}}=-0.82$
$\chi^{\mathrm{trig}}_{333}$	$-1.0\ \ \pm0.1$	$-\frac{2}{\sqrt{3}}=-1.15$
$\chi^{\mathrm{trig}}_{311}$	0.45 ± 0.05	$\frac{1}{\sqrt{3}}=0.58$

values for zinc blende expressed in trigonal coordinates. Comparing the relative magnitudes confirms that the effect of ordering on SHG is modest, except for very special directions like Fig. 1 at $\theta=0$. The analytical result for that signal is $\chi^{\mathrm{trig}}_{211}+\sqrt{2}\chi^{\mathrm{trig}}_{311}$, which is zero for disordered zinc blende.

We can make further use of reflection SHG to study CuPt ordered structures. $Ga_{1-x}In_xP$ grown on nonvicinal (001) substrates is known to form domains that are randomly oriented along $[1\ 1\ 1]^{\mathrm{cub}}$ or $[1\ 1\ 1]^{\mathrm{cub}}$. Since the domains are small compared to optical wavelengths,[12] we expect SHG to be determined by the symmetry of the composite film,[13] group $2mm$. Measurements normally incident to the $(0\ 0\ 1)^{\mathrm{cub}}$ surface should detect zero bulk signal because of the XY^{cub} inversion symmetry. We have measured a double-variant sample in this way, and the signal was more than an order of magnitude smaller than the order-induced contribution of single-variant $Ga_{1-x}In_xP$. A fourfold rotation symmetry suggests that the residual signal originates from surface SHG.[14]

In conclusion, we have used resonant reflection SHG to uniquely determine the point group of ordered $Ga_{1-x}In_xP$. Experimental conditions are found for a signal originating purely from the order-induced symmetry breaking. The four independent elements of $\chi^{(2)}$ are measured relative to GaAs, with sufficient accuracy to reproduce in Fig. 3(b) the rotation-dependent measurements on $Ga_{1-x}In_xP$, shown in Fig. 3(a).

We would like to thank H. M. Cheong and Y. Zhang for valuable discussions, and C. Kramer for the growth of the samples. This work was supported by the Office of Energy Research, Materials Science Division of the DOE, under Contract No. DE-AC36-83CH10093.

[1] H. M. Cheong, F. Alsina, A. Mascarenhas, J. F. Geisz, and J. M. Olson, Phys. Rev. B **56**, 1888 (1997).

[2] J. S. Luo, J. M. Olson, K. A. Bertness, M. E. Raikh, and E. V. Tsiper, J. Vac. Sci. Technol. B **12**, 2552 (1994).

[3] Y. Zhang, B. Fluegel, A. Mascarenhas, J. F. Geisz, J. M. Olson, F. Alsina, and A. Duda, Solid State Commun. **104**, 577 (1997).

[4] P. Ernst, C. Geng, F. Scholz, and H. Scheizer, Appl. Phys. Lett. **67**, 2347 (1995).

[5] B. Fluegel, Y. Zhang, H. M. Cheong, A. Mascarenhas, J. F. Geisz, J. M. Olson, and A. Duda, Phys. Rev. B **55**, 13 647 (1997).

[6] T. Kanata, M. Nishimoto, H. Nakayama, and T. Nishino, Appl. Phys. Lett. **63**, 512 (1993).

[7] R. G. Alonso, A. Mascarenhas, G. S. Horner, K. A. Bertness, S. R. Kurtz, and J. M. Olson, Phys. Rev. B **48**, 11 833 (1993).

[8] P. Grossmann, J. Feldmann, E. O. Göbel, P. Thomas, D. J. Arent, K. A. Bertness, and J. M. Olson, Appl. Phys. Lett. **65**, 2347 (1994).

[9] J. F. Nye, *Physical Properties of Crystals* (Clarendon, Oxford, 1985).

[10] J. I. Dadap, X. F. Hu, M. H. Anderson, M. C. Downer, J. K. Lowell, and O. A. Aktsipetrov, Phys. Rev. B **53**, R7607 (1996).

[11] R. Wirth, A. Moritz, C. Geng, F. Scholz, and A. Hangleiter, Phys. Rev. B **55**, 1730 (1997).

[12] C. S. Baxter, W. M. Stobbs, and J. H. Wilkie, J. Cryst. Growth **112**, 373 (1991).

[13] A. Mascarenhas, Y. Zhang, R. Alonso, and S. Froyen, Solid State Commun. **100**, 47 (1996).

[14] H. W. K. Tom, T. F. Heinz, and Y. R. Shen, Phys. Rev. Lett. **51**, 1983 (1983).